Hardware and physical integration guideline PCR Sensor A111

User Guide

Hardware and physical integration guideline PCR Sensor A111

User Guide

Author: Acconeer

Version 1.5: 2022-03-07

Table of Contents

1 Introduction

This document aims to provide general guidelines for the hardware and physical integration of the Acconeer A111 radar sensor. The A111 sensor is a fully integrated 60 GHz radar including the transmitter and receiver antenna. The Tx/Rx antenna is a folded-dipole type and the E-plane and H-plane of the antennas are indicated in Figure 1. The radiation pattern of the radar transceiver can be found in the A111 datasheet.

The provided guidelines aim to optimize the radar sensor performance when integrating it into your host product.

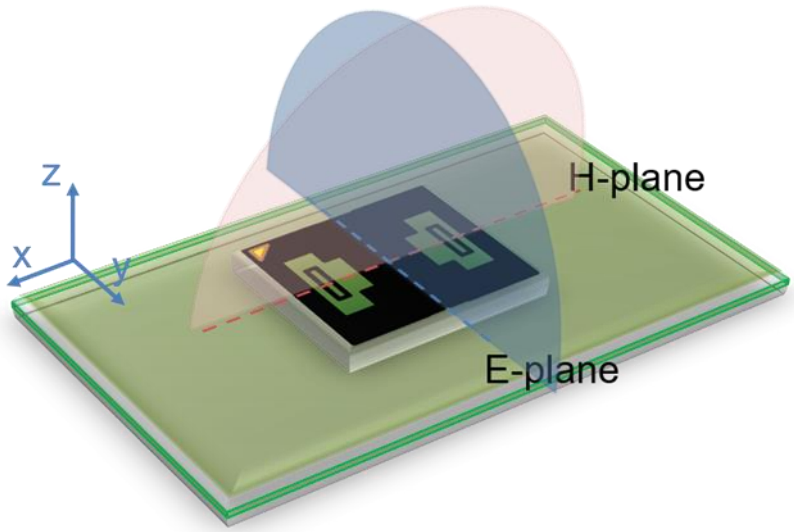

Figure 1. Sensor mounted on a printed circuit board (PCB). E-plane and H-plane are highlighted with blue and red color, respectively.

1.1 Radar loop equation

Consider a signal transmitted through free space to a radar target located at distance R from the radar. Assume there are no obstructions between the radar and the radar target, and the signal propagates along a straight line between the two. The channel model associated with this transmission is called a line-of-sight (LOS) channel. For the LOS channel, the corresponding received reflected power from a radar target, i.e. the signal to noise ratio (SNR), can be defined as

$$SNR = C\sigma\gamma\frac{1}{R^4} \quad (1)$$

R is the distance of the radar to the target, C is the radar loop gain, including both the transmitter and receiver chain (two-ways signal path), σ is the Radar Cross Section (RCS) of the scattering object and γ determines the reflected power of the object's material. RCS depends on the roughness, size and shape of the scattering object. Moreover, SNR depends on the sensor profile setting. A comprehensive explanation of the sensor profiles can be found in Acconeer's Radar Sensor Introduction.

1.2 Radar loop radiation pattern

When characterizing the gain, we refer to the radar loop gain defined in the radar equation section. Figure 2 shows the radar setup configuration for the radar loop radiation pattern measurement. The reflector which in this case is a circular trihedral corner (radius of 3.8 cm) is located at the far-field distance from the sensor (1 m). The far-field distance can be determined by the aperture of the sensor and the radar target.

$$R_{\text{farfield}} > \frac{2A^2}{\lambda} \tag{2}$$

where A is the largest dimension of either the sensor or the radar target. Envelope service can be used to collect the reflected power at the fix distance from the radar target at different rotation angle. The amplitude variation stated in the document shows one direction (TX or RX side). The radar loop gain (RLG) is in fact twice the amplitude value. This is applicable for all the figures which state the amplitude variation of the radome and the lens.

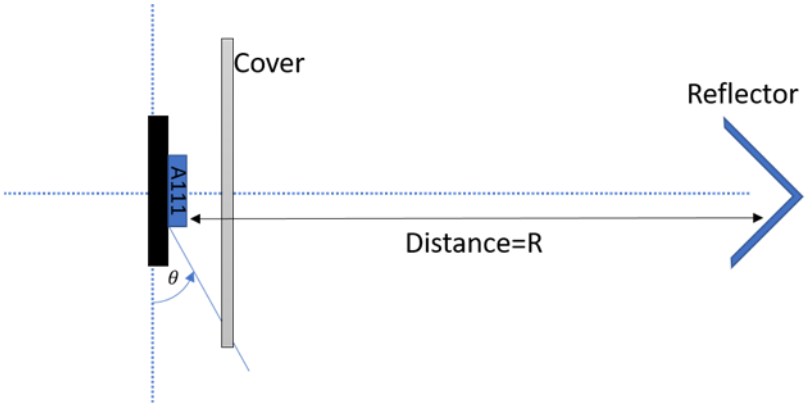

Figure 2. Measurement setup for radar loop radiation pattern.

2 HW Integration - Schematics

2.1 Power

The A111 is powered by 1.8 V and all the control signals and the SPI interface are 1.8 V pins. It must therefore be ensured that all host MCU pins connected to the A111 are at 1.8 V. If this is not the case, level-shifters must be used in between the A111 and the host MCU.

As mentioned in the power consumption summary of the A111 datasheet, the A111 consumes typically 66 µA when the ENABLE pin is set low. If the leakage current is to be even further reduced, the power to the A111 must be switched off. It can be achieved either by using a low-leakage power regulator with an enable/disable function (if 1.8 V is not available in the system) or a low-leakage power switch in between the two 1.8 V domains. In both cases, a control signal, PMU_ENABLE, is needed. See Figure 3 for details.

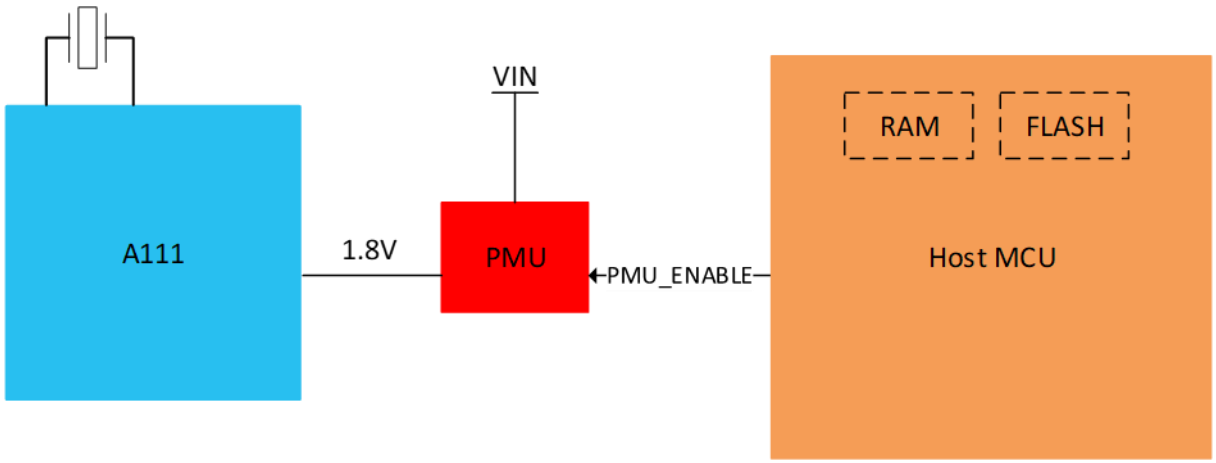

Figure 3. Block diagram of how to connect a Power Management Unit for controlling the 1.8V to the A111.

If the power to the A111 is switched off in between sweeps it is important that the control signals and SPI interface are pulled low during this time, otherwise reverse leakage will occur via the ESD diodes in the A111. If it is not possible to set the SPI interface in such a state (either via SW or by configuring any level-shifters that might be used in the design), the problem can be solved by adding a power switch only to VIO1 and VIO2. This way the leakage will be significantly lower than 66 µA, but the control signals and SPI interface of A111 will still be supplied by 1.8 V and thus no reverse leakage will occur. See Figure 4 for details. The Acconeer High Performance Module shows how to integrate a power switch into the design, refer to the XM112 datasheet.

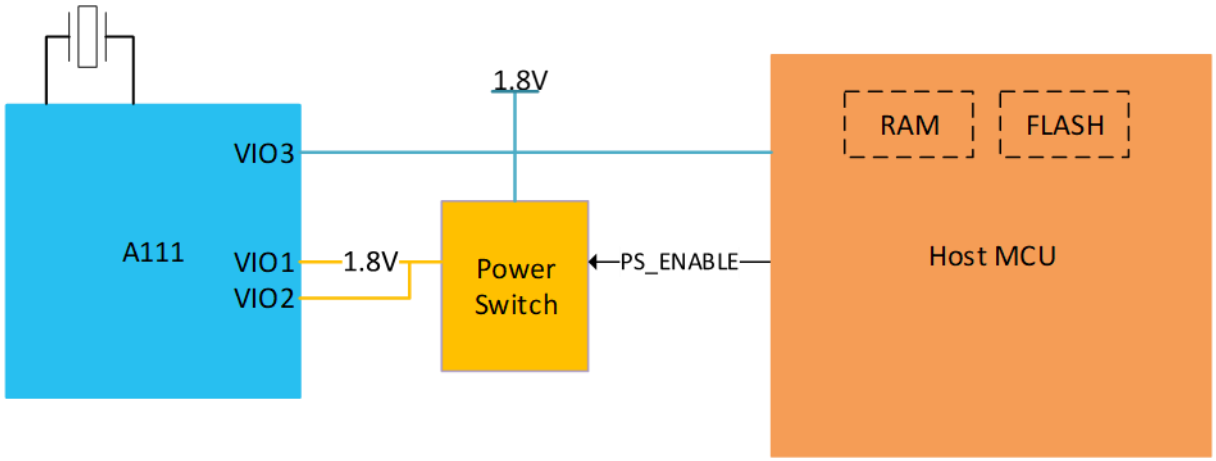

Figure 4. An example of how to connect a power switch to reduce the leakage current when A111 is powered off.

2.2 SPI Interface

To optimize signal integrity of the SPI bus, it is recommended to route the SPI bus with as short as possible trace lengths with an adjacent ground plane.

3 PCB layout

This chapter describes means of optimizing the sensor performance by properly designing the printed circuit board (PCB).

3.1 Sensor ground plane size

To maximize the radar loop gain and minimize impact on radiation pattern, it is recommended that the top PCB layer is a filled copper layer with minimum amount of routing close to the sensor. Figure 5 shows the relative loss in RLG as a function of ground plane size, assuming a solid square ground plane and the sensor placed at the center. As the ground plane size is increased, the RLG increases because of increased antenna directivity. However, the RLG doesn't increase monotonically with ground plane size due to constructive and destructive interference.

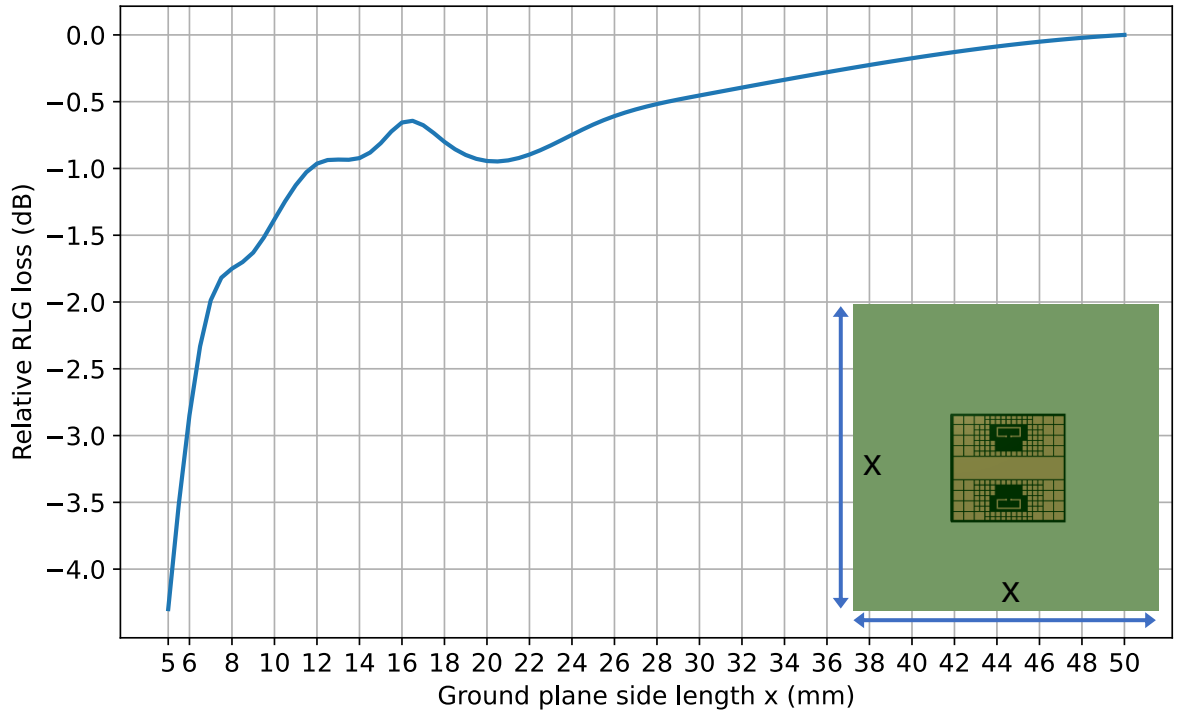

Figure 5. Simulated relative radar loop gain as a function of ground plane side length (x). Ground plane is a solid square ground plane without routing.

In terms of regulatory compliance, any openings in the ground plane inside the A111 BGA footprint must be significantly smaller than the wavelength of the radiation that is being blocked, to effectively approximate an unbroken conducting surface.

3.2 Impact of PCB routing and nearby components

The radar sensor can be integrated with other components on the same layer if required in compact designs. However, the radiation pattern is most sensitive to the ground plane area just outside the sensor. Therefore, if maximum directivity is important, place other components on the opposite side of the sensor or keep component count and routing to a minimum close to the sensor footprint. Vias should be placed as close as possible to the pads to maximize the ground plane area as shown in Figure 6. It is also recommended to minimize copper clearance for traces, vias and pads. The ground plane area inside the

footprint will have a lesser impact on the directivity and therefore some vias and short traces are preferably placed there while still satisfying regulatory compliance.

If the PCB assembly process allows, connect all ground pads without thermal reliefs as shown in Figure 6 a-b. Figure 7 shows the simulated relative RLG for the different routing examples in Figure 6. Omitting thermal reliefs as in Figure 6a can increase the boresight RLG by approximately 2 dB, provided there are no other interfering components or PCB traces close to the sensor. A small drop of approximately 0.5 dB is seen when placing decoupling capacitors (metric 1005) as shown in (Figure 6b).

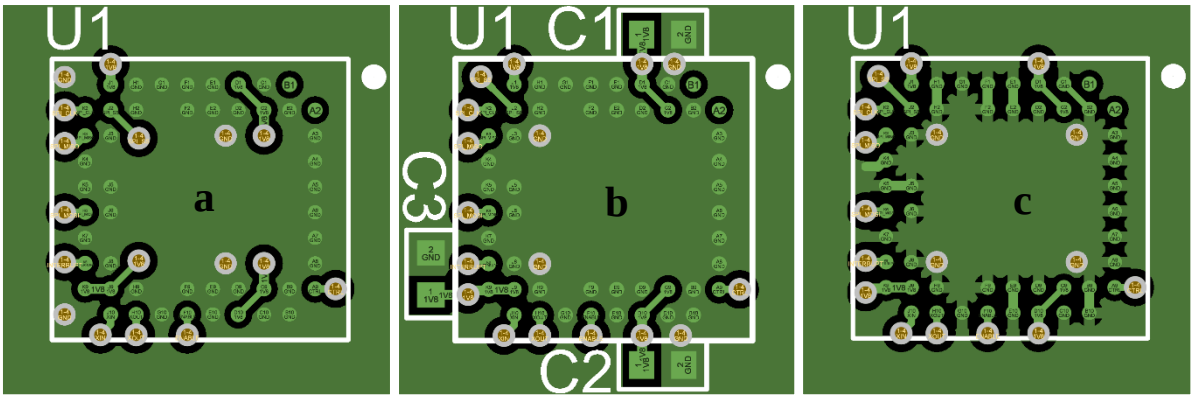

Figure 6. A111 routing examples with vias placed close to sensor for maximizing ground plane size. (a) Without GND thermal reliefs, (b) with decoupling capacitors and without GND thermal reliefs, (c) with GND thermal reliefs. Trace to copper clearance is 0.127 mm (5 mil) and via pad diameter is 0.45 mm.

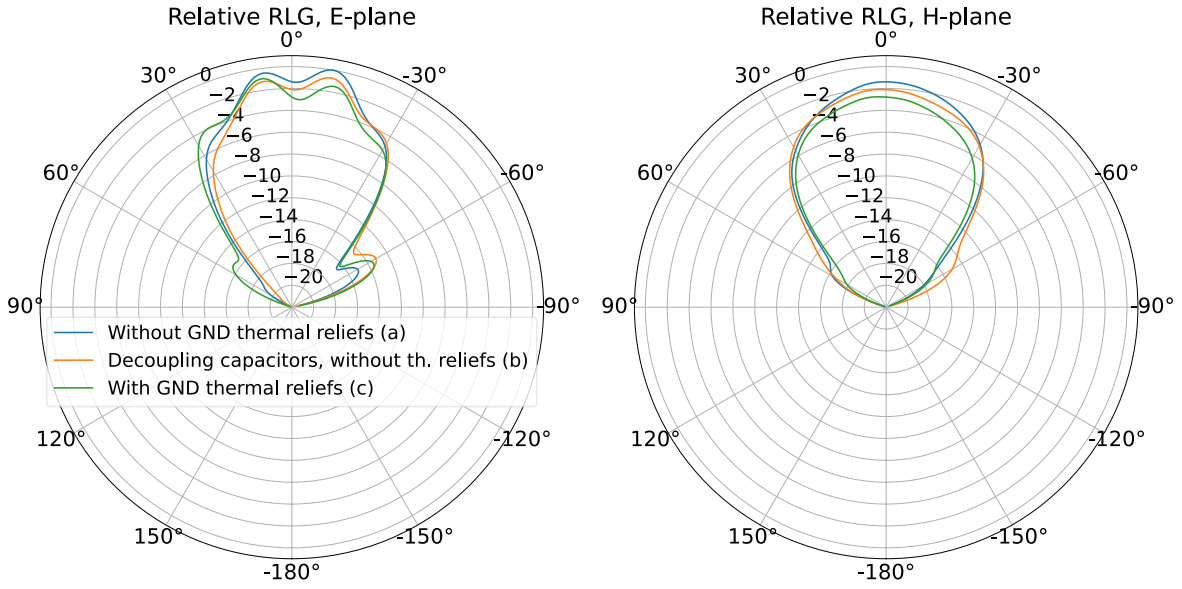

Figure 7. Relative RLG loss with and without A111 thermal reliefs.

Example PCB designs can be found on the Acconeer developer page [1].

For designs requiring larger components close to the sensor, a tapered shielding wall can be designed as shown in Figure 8.

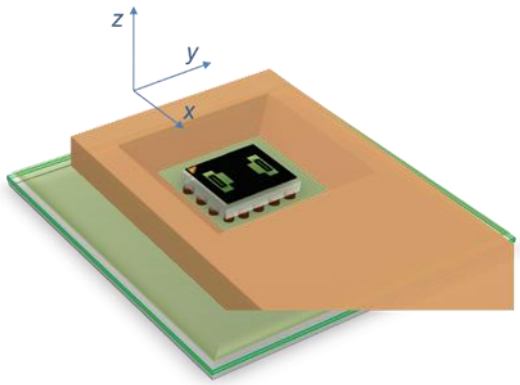

Figure 8. Tapered shield wall designed to prevent unwanted reflections from components placed close to the radar sensor.

3.3 Impact of conformal coating

Conformal coating may be used to protect the sensor and other electronic components from environmental factors such as moisture, dust, and chemicals. Conformal coatings are typically made of polymeric materials with dielectric constants typically in the range $\varepsilon_r < 4$. Depending on the coating material properties and layer thickness, one can expect a drop in the sensor's radar loop gain (RLG). This gain drop is due to three factors;

1. Offset in antenna resonance frequency as the antenna becomes electrically longer.
2. Reflection and refraction loss due to the interface between the sensor and the coating.
3. Dielectric loss in the coating material. This can usually be neglected for thin coating layers (e.g. <200 µm).

Figure 9 shows the simulated relative radar loop gain (RLG) after a linear lossless ($\tan(\delta) = 0$) isotropic coating has been added to all sides of the radar sensor. As the coating thickness increases and/or the dielectric constant increases, the RLG decreases. The loss is however non-monotonic, and this is due to constructive and destructive interference depending on the coating thickness.

The loss due to antenna resonance frequency offset can be seen in Figure 10 where the maximum gain is shifted in frequency. This means that, as the radar signal is a wideband signal, the resulting loss in SNR can be expected to be somewhat less than what is estimated in Figure 10.

If it is critical to obtain the maximum gain, it is recommended to use a thin coating layer (< 40 µm) with low dielectric constant and loss factor. However, as many coating materials are not well characterized at mm-wave frequencies it may be best analyzed by performing actual tests.

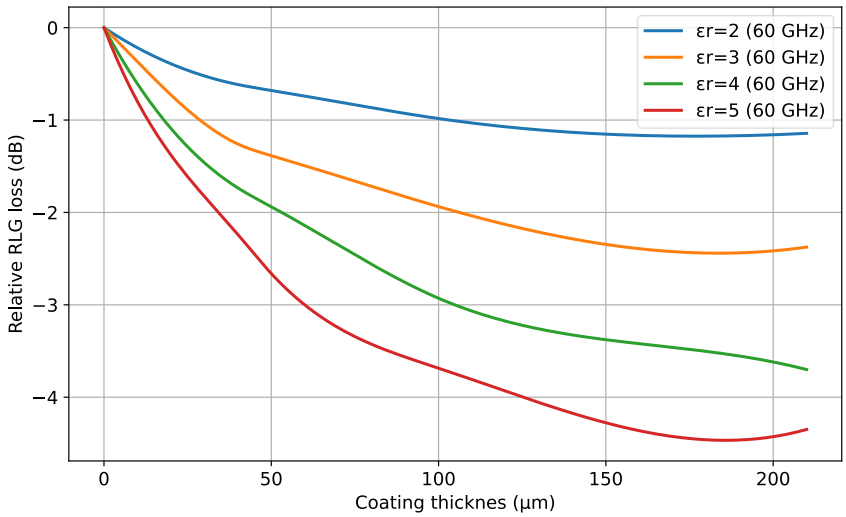

Figure 9. Simulated impact of lossless dielectric conformal coating on radar loop gain (RLG) at center frequency (60.5 GHz).

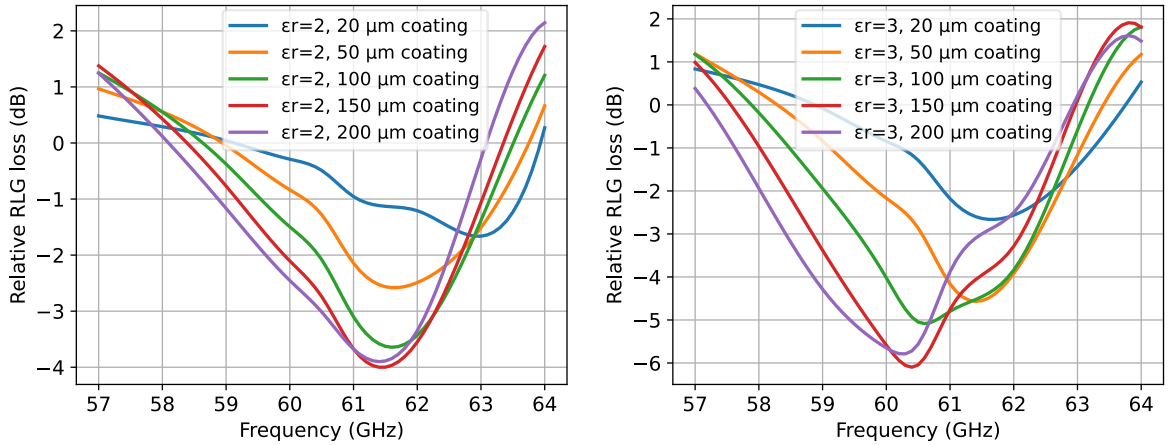

Figure 10. Simulated impact of conformal coating with ε_r =2 and ε_r =3 for different thicknesses.

3.4 Sensor underfill

Underfills can be used to fill the gap between the sensor package and PCB. The sensor underfill material should be chosen to have as low dielectric constant and loss tangent as possible. Dielectric constant determines the reflectivity of the medium and loss tangent indicates the dissipation effect of the material and both are frequency dependent.

4 Physical Integration

EM waves can interact with the objects and the media in which they travel. As EM waves propagate, they can be reflected, refracted, or diffracted. These interactions cause the radar pulse to change the direction and to reach the areas which would not be possible if the radar pulse travelled in a direct line.

This chapter provides the integration guidelines for simplified sensor cover scenarios. In any case, it is important to carefully design and characterize the integration to ensure that the desired performance is obtained. The radiation pattern presented in the A111 datasheet (developer.acconeer.com), shows the sensor performance when integrated in free space.

4.1 Radome integration

A radome is a structural enclosure that protects a radar assembly. Radomes are generally made of materials which are mainly characterized by their dielectric properties. Dielectric materials have a characteristic impedance of

$$Z_d = \frac{Z_0}{\sqrt{\epsilon_r}}$$

where ϵ_r is the dielectric constant relative to the free space and Z_0 is the wave impedance in free-space.

$$Z_0 = \sqrt{\frac{\mu_0}{\varepsilon_0}} = 377\ \Omega$$

When an EM wave hits a dielectric material at a normal incident angle, the reflection coefficient is defined as

$$\Gamma = \frac{Z_d - Z_0}{Z_d + Z_0} = \frac{\sqrt{\varepsilon_0} - \sqrt{\varepsilon_r}}{\sqrt{\varepsilon_0} + \sqrt{\varepsilon_r}}$$

The transmission coefficient is defined as T = 1 + Γ. It is important to select dielectric materials for the radome such that the reflection coefficient has a low value. Therefore, a low dielectric constant material will minimize the reflections and reduce the impact on the radiation pattern and insertion loss. Typically, radomes are made of plastic and the dielectric constant of common plastic (ABS, PC, Teflon, PP) is less than 3, therefore, reflection coefficient for plastic materials is usually low. To further optimize the radome integration, shape of the radome, distance to the radar and the thickness of the radome needs to be considered in the design.

Figure 11 shows a scenario where a 1mm thick radome made of ABS plastic is placed at different distances, D, from the radar. The amplitude variation of the reflected waves from the radar target can be seen in the measured results shown in Figure 12. The variation of the amplitude is explained by the standing wave phenomena. The transmitted wave (indicated as blue in Figure 13) travels in the air medium until it reaches the second medium (plastic cover). Depending on the properties of the second medium, part of the energy will be transmitted through the medium and part of it will be reflected. The reflected pulse (indicated as yellow in Figure 13) will travel back to the PCB and be reflected again (indicated as red in Figure 13). Depending on the distance D, the transmitted wave and the reflected pulse can add up coherently or noncoherently. The maximum and minimum occur at multiples of the half wavelength of the radar pulse. The impact of the pulse length is visible in the measurement results (Figure 12). When the distance D gets larger than the pulse length, the standing wave disappears.

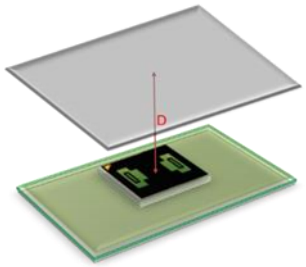

Figure 11. Placement of the radome in relation to the sensor.

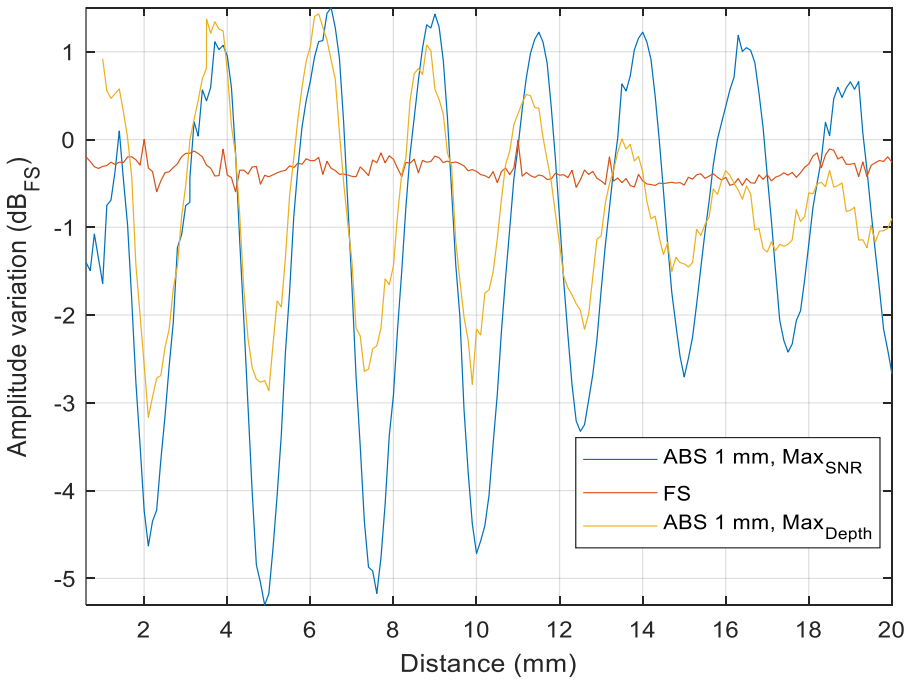

Figure 12. Measured reflected power from the target versus the radome to sensor distance for two different service profiles, Profile 2 (MaxSNR) and Profile 1(MaxDepth). Amplitude is nomalized by the maximum value of Free Space. Amplitude variation is stated in one direction (Tx or Rx side). For Radar Loop Gain (RLG) the values will be doubled.

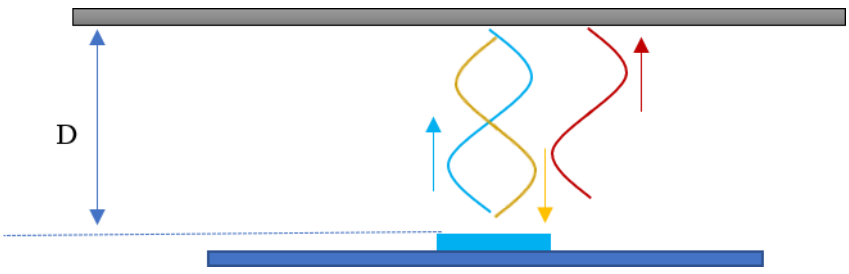

Figure 13. Illustration of the transmitted pulse and the reflected pulses (from plastic cover and the PCB).

4.2 Radome thickness

When an EM wave travels in a dielectric material, its effective propagation speed and the wavelength will change depending on the dielectric material:

$$c_{\text{eff}} = \frac{c_0}{\sqrt{\epsilon_r}}, \lambda_{\text{eff}} = \frac{\lambda_0}{\sqrt{\epsilon_r}}$$

where ϵ_r is the dielectric constant of the material, c_0 is the speed of light in free space, i.e. 3×10^8 and λ_0 is the free space wavelength ($\lambda_0 = 5$ mm for A111).

Reflections happens at the air-dielectric interfaces and the thickness of the dielectric medium determines the phase shift of the reflected wave from dielectric-air interface. Figure 14 shows a simplified model of the transmission and reflections of the waves between air-dielectric. Reflections from the second bounce and above are neglected in this model. When the wave impinges the air-dielectric interface, part of it reflects (r_{01}) and part of it transmits (t_{01}). The thickness of the dielectric material will cause the wave to shift phase by:

$$\theta = \frac{2\pi}{\lambda_{\text{eff}}} h$$

where h is the thickness of the dielectric. When the wave reaches the dielectric-air interface ($t_{01}e^{-j\theta}$), another transmission ($t_{10}t_{01}e^{-j\theta}$) and reflections ($r_{10}t_{01}e^{-j\theta}$) happens. Notice that the wave will have a sign change when the reflection happens, $r_{10} = -r_{01}$. At the lower dielectric-air interface, the amplitude of the wave is $-r_{01}t_{01}e^{-2j\theta}$, where the wave has traveled a distance of $2h$.

If we assume a half-wavelength-thick radome, the round trip of the wave inside the radome will introduce a 360-degree phase shift. Hence, the reflected wave into the air has a $-r_{01}t_{10}t_{01}$ amplitude. In this case, the reflected waves , $t_{10}t_{01} \approx -r_{01}$ and r_{01} will cancel out. Therefore, to minimize the reflections, the thickness of a single layer radome should be half-a-wavelength or a multiple of it.

$$h_{\text{optimum}} = n\frac{\lambda_{\text{eff}}}{2}, \quad n = 1,2,3, \ldots$$

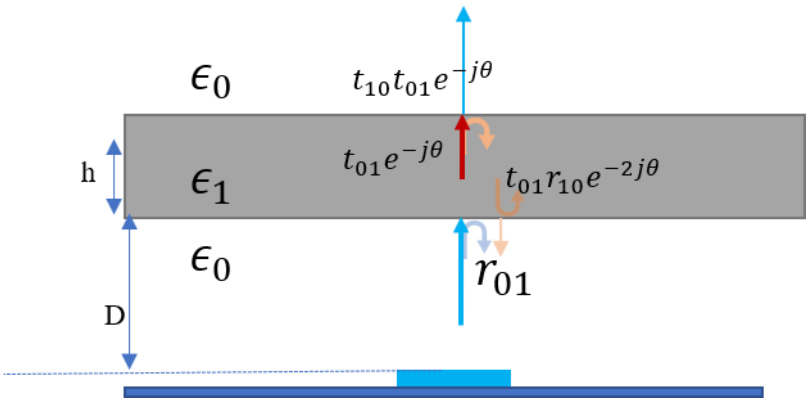

Figure 14. Incident wave impinging the radome at the normal incident angle. Transmission and reflection of the wave at the interfaces of two mediums.

As an example, a plastic sheet made of ABS with different thicknesses was selected for the test measurement. If we assume dielectric constant of ABS to be 2.6 (the dielectric constant can vary depending on the vendor), the thickness of the half-a-wavelength-thick radome is calculated to be

$$h = \frac{\lambda_{eff}}{2} = 1.55\ mm$$

Figure 15 shows the amplitude variation of the reflected wave from the radar target when the distance between the sensor and the radome is varied for different radome thicknesses. A thickness of 1.6 mm, which is very close to the thickness of half-a-wavelength, has the minimum impact on the amplitude variation. It is worth to mention that when the thickness is set to quarter-of-a-wavelength, the amplitude variation becomes maximum. When the radome thickness is set to quarter-of-a-wavelength, the round trip of the wave inside the radome leads to a 180° phaseshift.

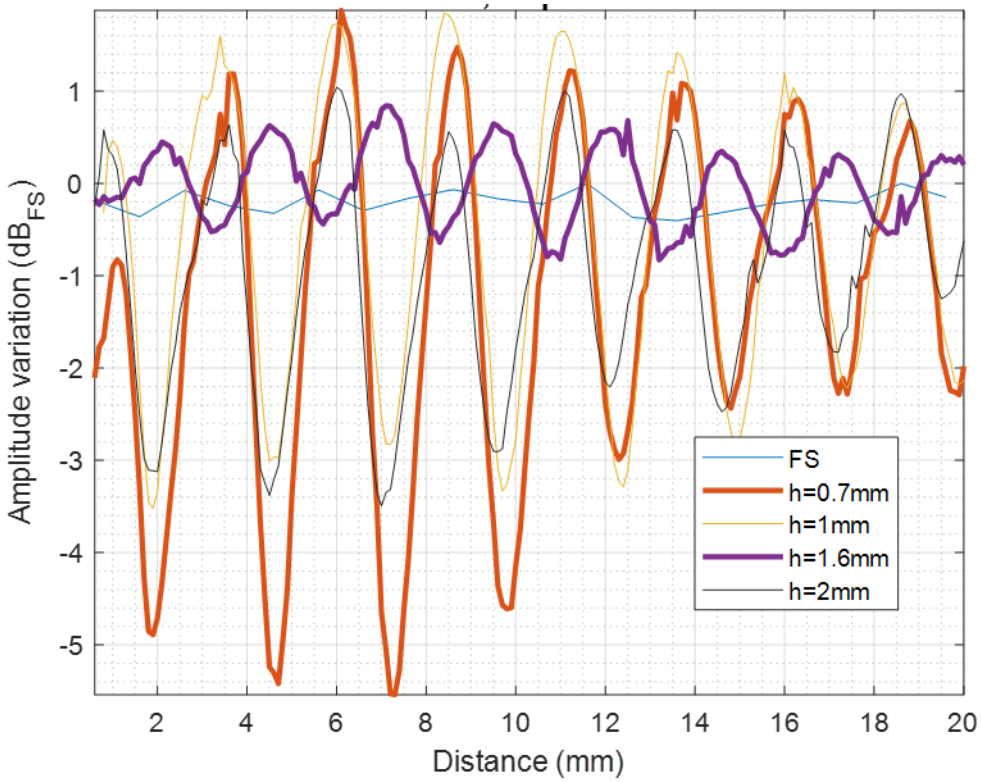

Figure 15. Impact of the thickness of the radome (made of ABS) on the reflected amplitude variation. The amplitude is normalized to maximum value of the Free Space (FS). Profile set to Profile 2. Amplitude variation is stated in one direction (Tx or Rx side). For Radar Loop Gain (RLG) the values will be doubled.

If absolute measurements are required for a certain use case, it is advised that an additional offset is added to the distance measurement. The reason for this offset is that the propagation delay caused by the radome must be compensated. This additional offset is obtained by making reference measurements, and it will also allow you to place the reference plane at the desired location for your product.

4.3 Radome distance

The reflected waves from the radome wall should be in-phase with the transmit waves, which leads to the optimum distance of

$$D_{optimum} = n\frac{\lambda_0}{2}, \quad n = 1,2,3, \ldots$$

The optimum distance is valid if the thickness of the radome is optimum as well. Otherwise, to have a minimum insertion loss on the received signal, the distance to the sensor should follow the marginal criteria below:

$$n\frac{\lambda_0}{4} - \delta < D < n\frac{\lambda_0}{4} + \delta, \quad n = 1,3,5, \ldots$$

In order to have zero insertion loss δ is determined to be 0.5 mm.

4.4 Impact on the radiation pattern

The radar loop radiation pattern of the integrated antennas will be affected by the dome that is put on top of the sensor. Figure 16 shows the measured radar loop pattern for three different materials, ABS plastic, gorilla glass and free space.

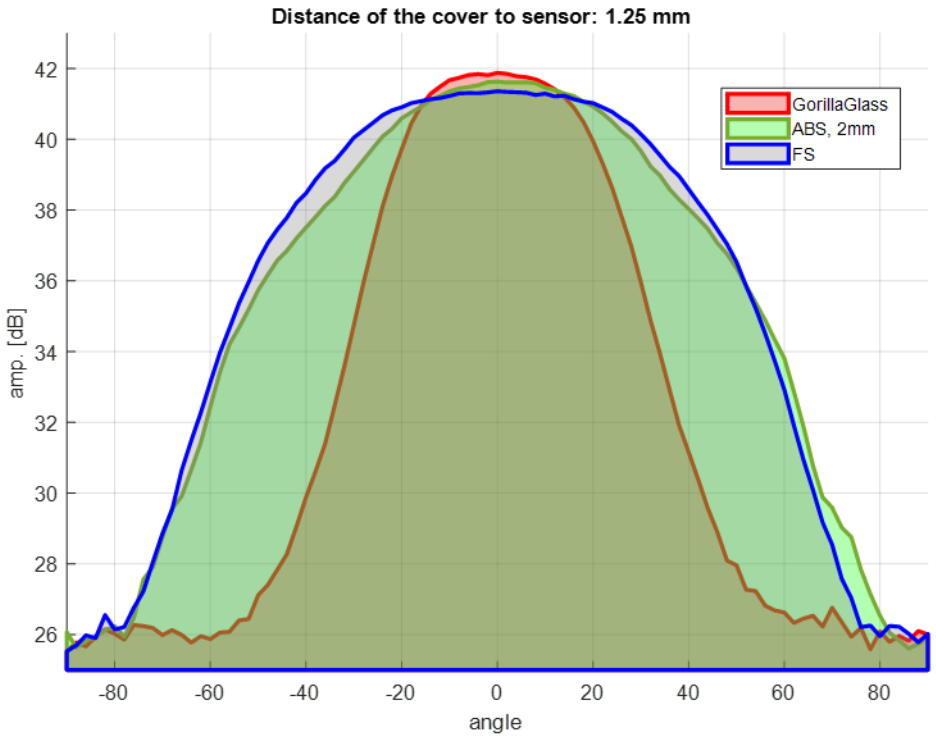

Figure 16. Impact of the different materials on the radiation pattern, H-plane. Amplitude is stated in one direction (Tx or Rx side). For Radar Loop Gain (RLG) the values will be doubled.

Figure 17 shows the radar radiation pattern when a radome made of ABS with 2mm thickness is placed at distances corresponding to the harmonics of the quarter-of-a-wavelength of the radar pulse. The reference case is FS (Free Space i.e. no cover). Since the radome thickness is not optimal, distances which correspond to odd harmonics of the quarter-of-a-wavelength have the minimum impact on the radiation pattern.

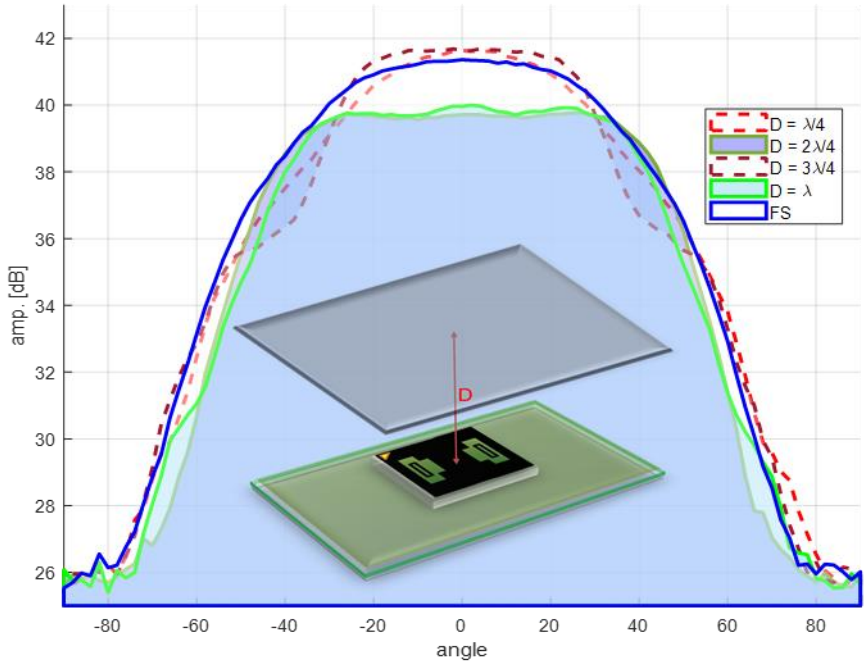

Figure 17. Impact of the radome-to-sensor distance on the radiation pattern (H-plane). Amplitude is stated in one direction (Tx or Rx side). For Radar Loop Gain (RLG) the values will be doubled.

It is not recommended to place the cover directly on the sensor. Figure 18 shows the radiation pattern on the H-plane when the cover (ABS plastic sheet) is located on top of the sensor. In comparison with Free Space, there is around 3 dB loss on both max. power and total radiated power for this case.

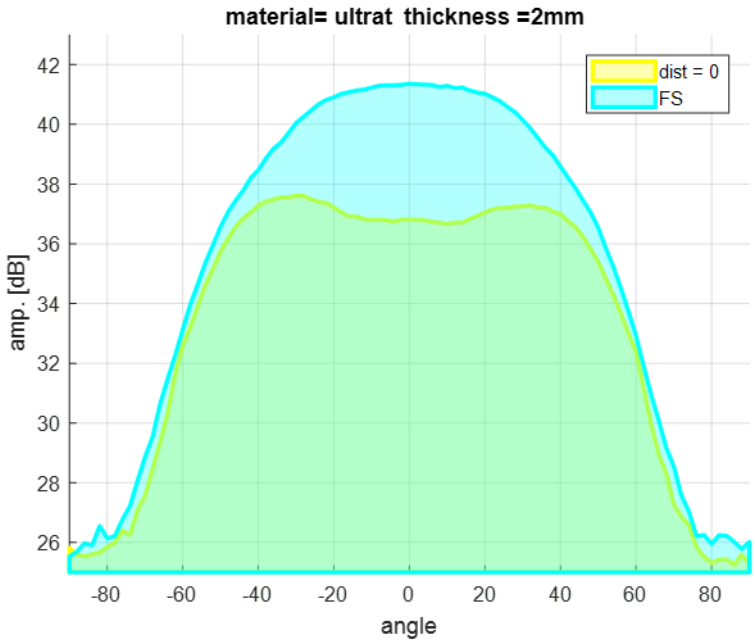

Figure 18. Radiation pattern on H-plane, cover placed directly on the sensor vs Free Space. Amplitude is stated in one direction (Tx or Rx side). For Radar Loop Gain (RLG) the values will be doubled.

4.5 Multi-layer radome integration

Radomes can also be constructed from a multi-layer dielectric. Particularly, where the thickness of a single layer dielectric is fixed, thus additional layer can be added to the radome which can act as an anti-reflection layer. Figure 19 shows the stack-up of a radome made of two dielectric layers and illustrates the scattering of waves in this scenario. In this scenario, the reflections formed at the interfaces of the different mediums can be cancelled if the condition below is satisfied:

$$r_{01} + t_{10}t_{01}r_{12}e^{-2j\theta} + t_{10}t_{21}r_{20}t_{12}t_{01}e^{-2j(\theta+\varphi)} = 0$$

The layer indicated with ϵ_2 dielectric constant is the main layer and the layer with the ϵ_1 dielectric constant is the matching layer. Depending on the degree of the freedom, one can find the optimum thickness or the optimum dielectric constant for the anti-reflection layer.

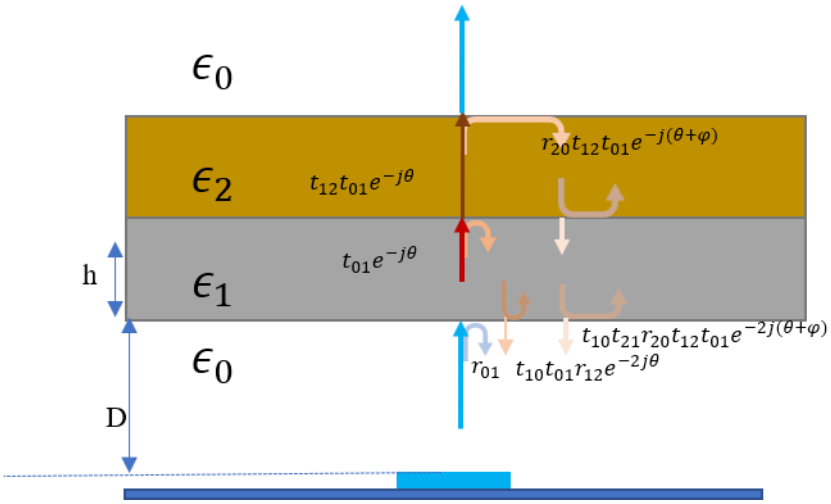

Figure 19. Illustration of the scattering waves for a two-layer radome.

Another approach is to use an EM simulation tool to find the characteristic of the anti-reflection layer. For example, Figure 20 shows a sensor integration scenario where the main layer of the radome is made of a special glass which has a high dielectric constant (~6-7). Therefore, the wave impedance mismatch between the glass and the air becomes large. To reduce the mismatch, a matching layer with a lower dielectric is applied between sensor and the screen. To find the optimum dielectric value of the matching layer, the dielectric constant is varied in the simulation. It can be seen from the results shown in Figure 21 that the gain drops at least 2 dB in case 1, compared to case 2 where the matching layer has a dielectric constant of 3.

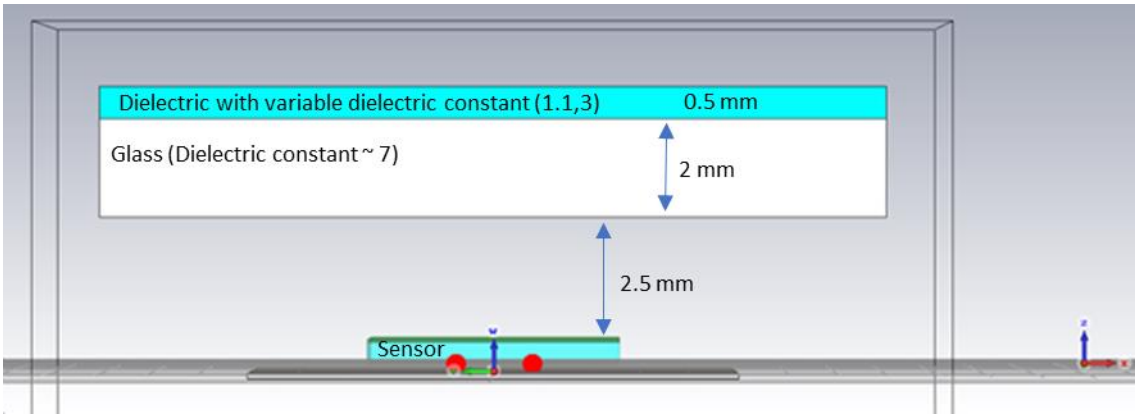

Figure 20. Simulation scenario: Sensor, air-gap, the matching layer and the screen.

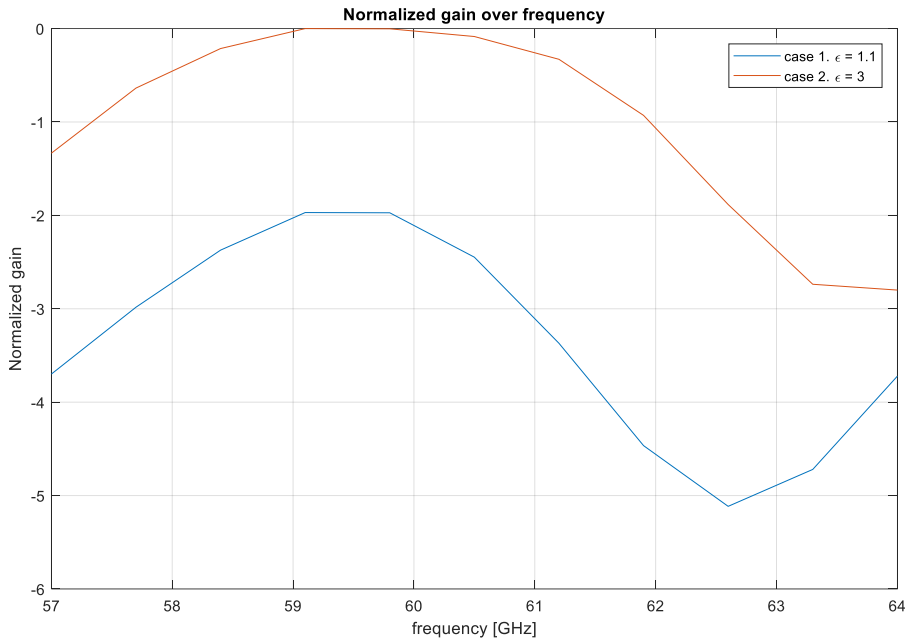

Figure 21. Normalized antenna gain (Tx or Rx antenna gain) where the matching layer dielectric constant is set to 1.1 and 3.

5 Physical Integration - Lens

For the applications where narrow beamwidth is required, additional lens antenna solution might be added to the sensor to achieve narrow beamwidth and high radar loop gain.

Dielectric lens antennas have the advantage that they can be more compact and weigh less than horn antennas and parabolic reflector antennas and they are easier to integrate to the product.

Acconeer have designed two type of lens to narrow the beamwidth and improve the radar loop gain. First is the hyperbolic lens and the second is based on the phase correcting plate which is called Fresnel Zone Plate (FZP) lens. The shape of the hyperbolic lens is chosen so that the rays passing through the lens originating from the focal point will have the same phase shift, i.e. they will depart in-phase from the lens. In case of the FZP lens, the radius of each subzone and its thickness, are chosen so that rays passing through the edges of neighboring subzones originating from the focal point have the same phase shift.

Figure 22 depicts how the transition from the spherical waves to planar waves is done by two different types of lens. The main parameters for the lens design are the focal point, dielectric constant of the lens, and curvature (hyperbolic, zone radius and thickness).

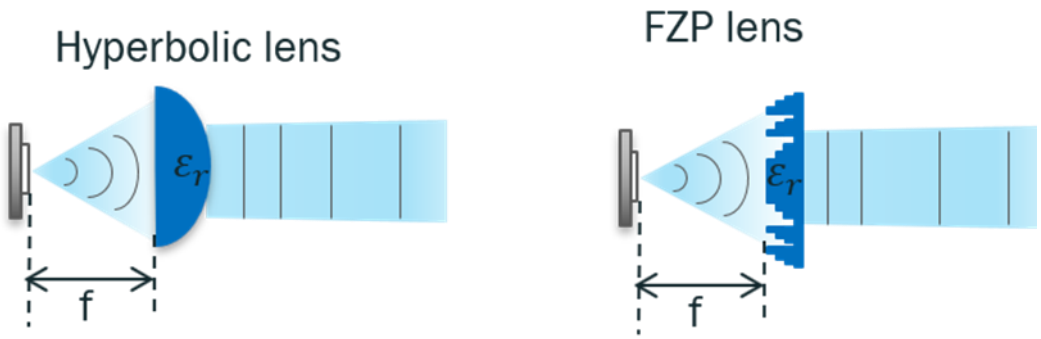

Figure 22. Hyperbolic and FZP lens located at the focal distance of the sensor.

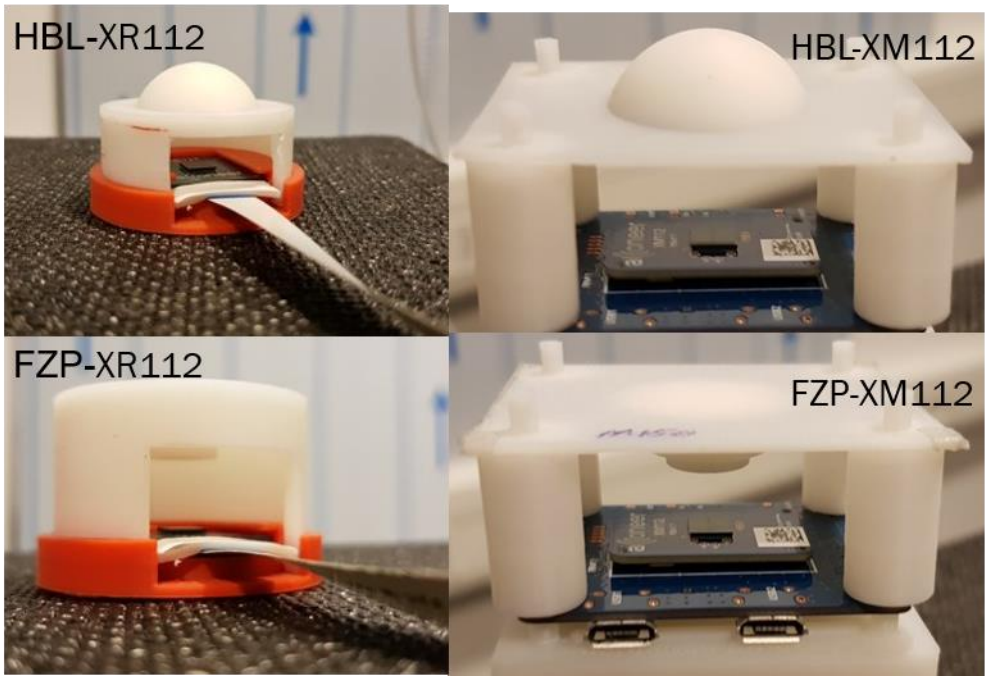

Figure 23. 3D-printed examples of the hyperbolic and FZP lenses. The material used for printing is ABS plastic.

5.1 Focal distance

Radar measurement was done to characterize the focal point of the lens. The reflected power from a fixed radar target was captured for different sensor-to-lens distance. The distance between the sensor and target is to be in the far-field region, i.e. radar-to-target distance > 1m.

Figure 24 shows the gain variation of the integrated lens with the radome with respect to the free-space scenario for the XM112 module (see Figure 23 for the prototype pictures). The maximum gain happens at 7.5 mm distance for both lenses. Other maxima happen every half-of-a-wavelength ($\frac{\lambda_0}{2} = 2.5$ mm). The gain oscillation is due to the constructive and non-constructive interference of the transmitted and reflected waves between the lens surface and the sensor. The optimal placement can vary depending on the radome design. The measured results for the XR112 radome (Figure 25) indicate that the maximum gain happens at 8 mm distance. This can be due to the reflections from the radome side walls which can create interference. Therefore, it is important for every radome design to characterize the focal distance to find the optimum distance.

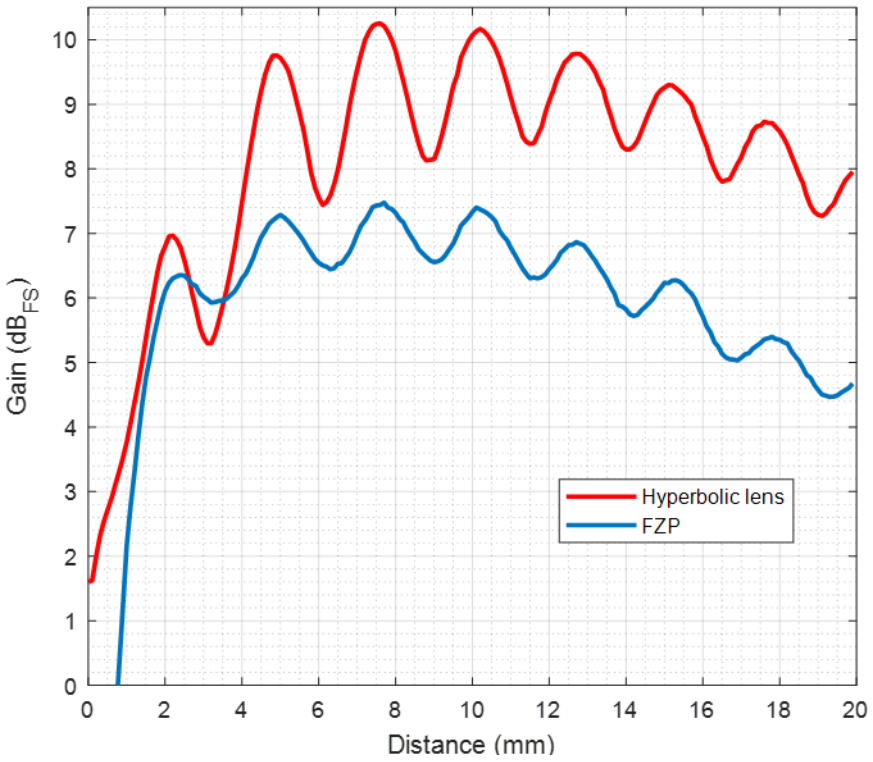

Figure 24. Gain variation of the lens versus the distance to the XM112 radome. The amplitude is normalized to Free Space (FS). Gain is stated in one direction (Tx or Rx side). For Radar Loop Gain (RLG) the values will be doubled.

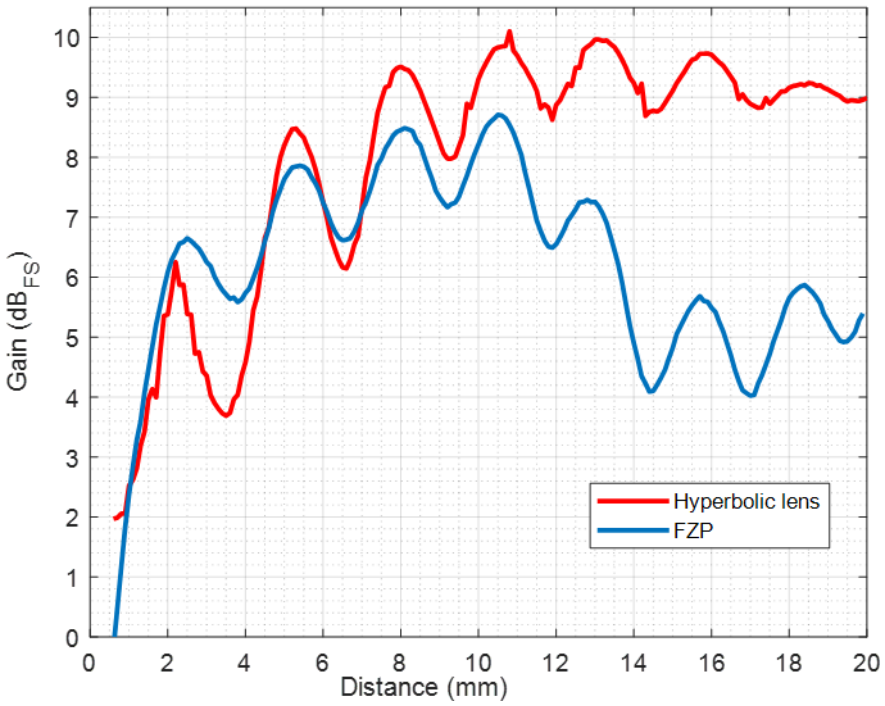

Figure 25. Gain variation of the HPL and FZP lens versus the distance to the XR112 radome. The amplitude is normalized to Free Space (FS). Gain is stated in one direction (Tx or Rx side). For Radar Loop Gain (RLG) the values will be doubled.

5.2 Radiation pattern

Two focal distances, $D_{sensor\text{-}lens}$= 2 and 8 mm, are chosen for characterizing the radar loop radiation pattern of the lenses. Figure 26 and Figure 27 show the measured radar loop pattern for free-space, HPL and FZP lenses for the selected focal distances. The measured gain is slightly lower than the expected values (refer to Figure 24). This is due to tolerances of the distance which impacts the gain. If one considers the FZP lens, the distance tolerance of +- 0.5 and +-1 mm results in 0.5- and 1-dB gain loss respectively.

For radar loop HPBW and RLG refer to module datasheets and the lens user guide. When the focal distance is set to 2 mm, the radiated beam is less directive compared to when the focal distance is set to 8 mm.

To conclude, when a new radome is designed, it is very important to characterize the integrated lens and radome to optimize the design for the targeted application.

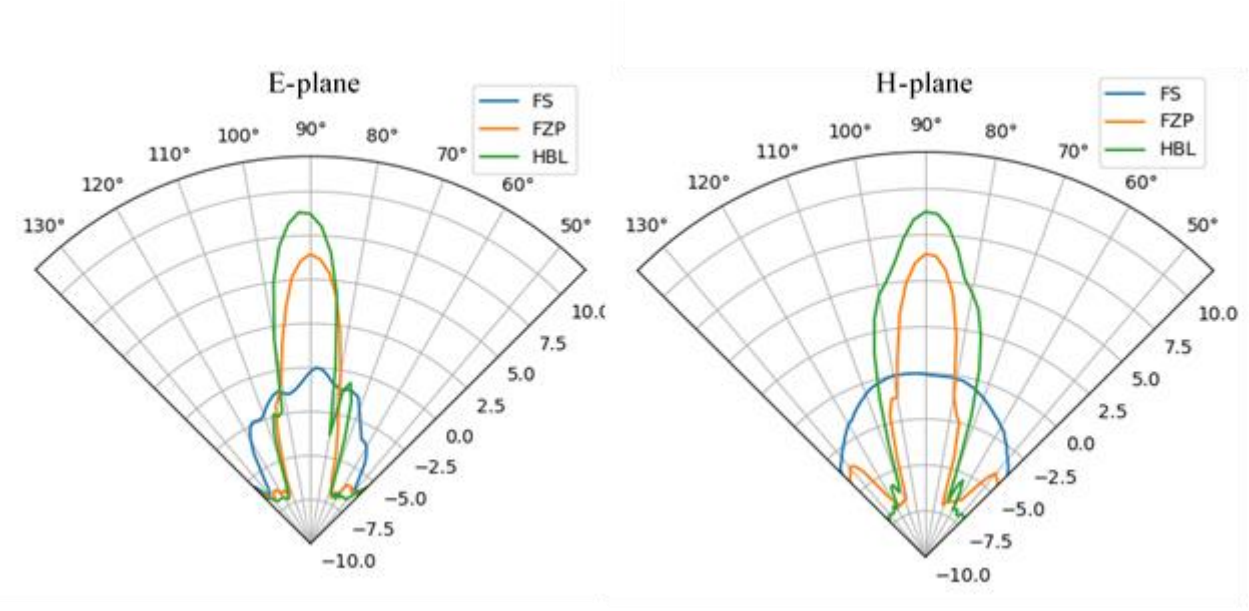

Figure 26. Radar loop radiation pattern of the sensor in Free Space and with lens. Distance from the lens to the sensor is set to 8 mm. Radius is in dB scale normalized to Free Space maximum gain. Gain value is stated in one direction (Tx or Rx side). For Radar Loop Gain (RLG) the values will be doubled.

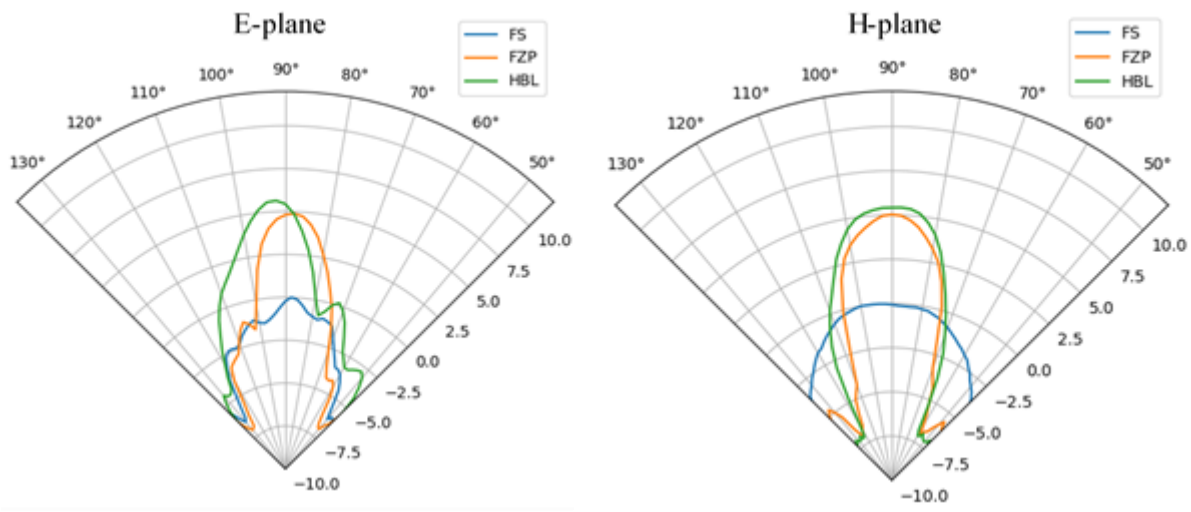

Figure 27. Radar loop radiation pattern of the sensor in Free Space and with lens. Distance from the lens to the sensor is set to 2 mm. Radius is in dB scale normalized to free space maximum gain. Gain value is stated in one direction (Tx or Rx side). For Radar Loop Gain (RLG) the values will be doubled.

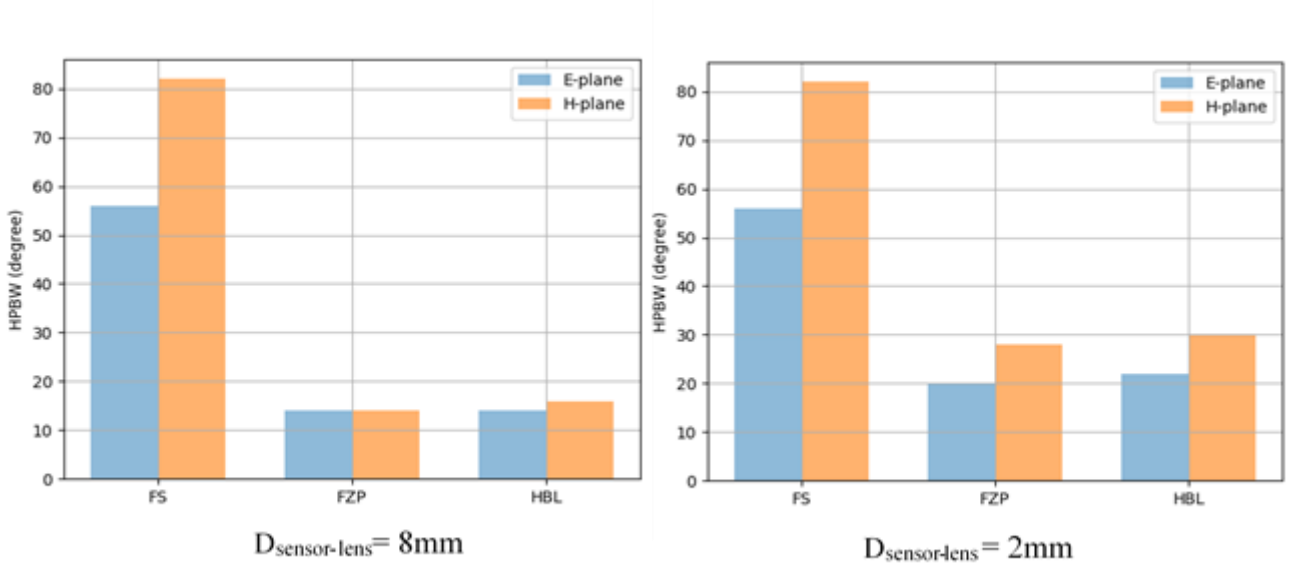

Figure 28. Half-power beam width for the FZP and hyperbolic lenses placed at a distance from the sensor of 8 mm and 2 mm respectively.

In Figure 29 the maximum gain of the lenses in the E-plane is shown for the two different focal distances.

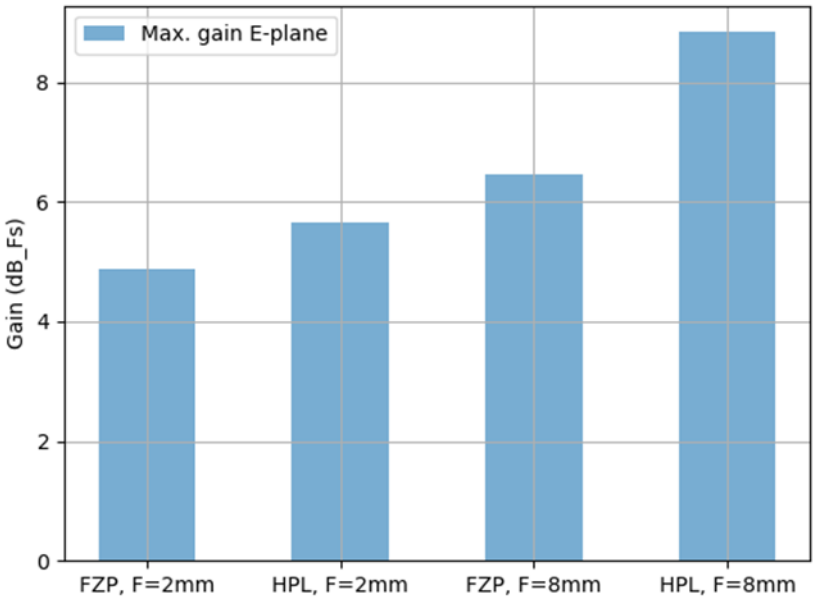

Figure 29. Gain of the FZP and hyperbolic lenses at E-plane for focal distances of 2 mm and 8 mm. Gain is stated in one direction (Tx or Rx side). For Radar Loop Gain (RLG) the values will be doubled.

5.3 FZP Lens Design

The FZP lens characterized in the previous chapters was made of ABS plastic. If other materials are to be used or if another focal point distance is needed, the dimensions of the FZP lens should be altered. In Figure 30, a detailed description of an FZP lens is shown, the radius and thickness for each step can be calculated by equations below:

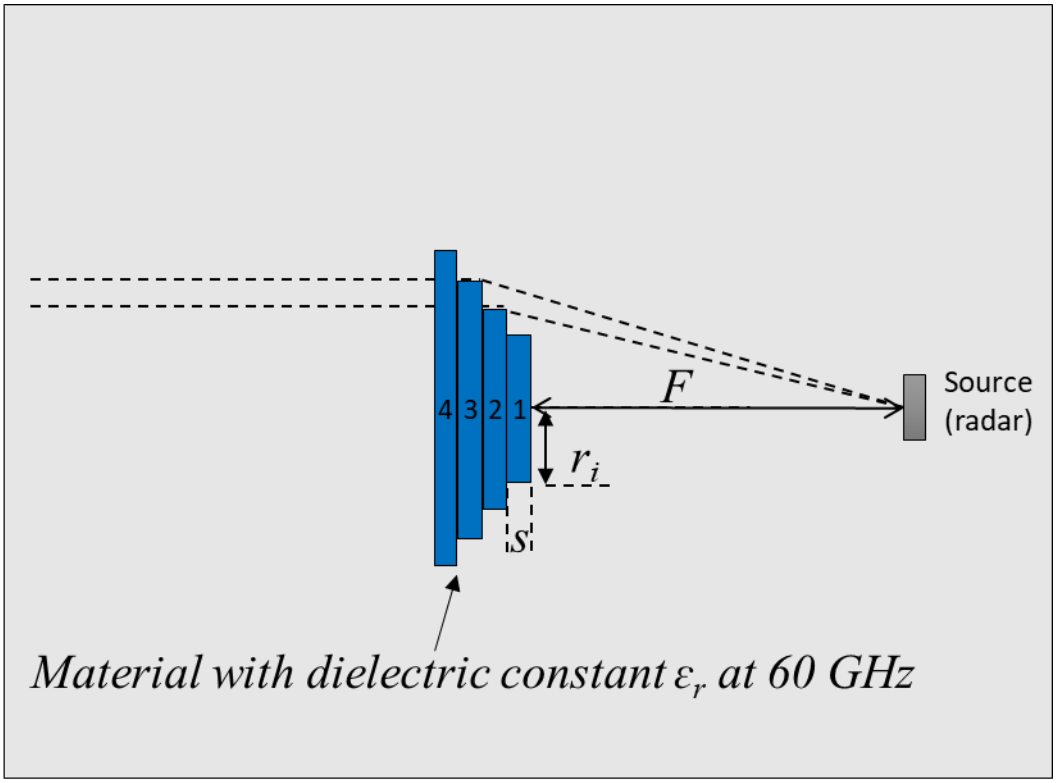

Figure 30. Detailed geometry of an FZP lens with quarter wavelength phase correction step.

$$r_i = \sqrt{\left(i\frac{\lambda}{p}\right)^2 + 2Fi\frac{\lambda}{p}} \qquad i = 1,2,3,4$$

$$s = \frac{\lambda}{p(\sqrt{\varepsilon_r} - 1)}$$

where r_i is the radius of each step, s is the thickness of each step, F is the focal point, p is the number of steps, λ is the wavelength in free-space (5 mm at 60 GHz), and ε_r is the dielectric constant of the chosen material at 60 GHz.

By using the equations mentioned above, one concludes that a four-step FZP lens in ABS-M30 plastic (ε_r = 2.48), with the focal point at 10mm, needs the following dimensions:

r_1 = 5.1mm

r_2 = 7.46mm

r_3 = 9.39mm

r_4 = 11.12mm

s= 2.17 mm

Total thickness of the lens: 4*2.17 = 8.7 mm

For further details regarding FZP and hyperbolic lens design, see [2].

6 Appendix A: Materials

Table 1. Measured dielectric constant and loss tangent of different materials at 60 GHz [3].

Material	Dielectric constant	Loss tangent
ABS-M30 (three-dimensional printed)	2.48	0.008
Acrylic glass	2.5	0.0118
Alumina	9.3	0.0013
Fused quartz	3.8	0.0015
MACOR	5.5	0.0118
PLA (three-dimensional printed)	2.85	0.014
Polyethylene	2.3	0.0003
Polypropylene	2.2	0.0005
Polystyrene (Rexolite)	2.5	0.0004
Teflon	2.2	0.0002

7 References

[1] "Acconeer developer page," [Online]. Available: https://developer.acconeer.com.

[2] K.-C. H. John Thornton, Modern Lens Antennas for Communications Engineering, Wiley-IEEE Press, 2013.

[3] S. R. Artem Boriskin, Aperture Antennas for Millimeter and Sub-Millimeter Wave Applications, Springer, 2017.

[4] "Acconeer Expolration Tool," [Online]. Available: https://acconeer-python-exploration.readthedocs.io/en/latest/sensor_introduction.html.

[5] "Acconeer A111 datasheet," [Online]. Available: https://developer.acconeer.com/download/a111-datasheet-pdf.

[6] "Acconeer PCR sensor A111 EVK hardware userguide," [Online]. Available: https://developer.acconeer.com/download/xc112_xr112-user-guide-pdf.

8 Revision

Date	Version	Changes
2019-11-13	1.0	Original version
2020-07-02	1.2	Comments on the gain values
2020-11-25	1.3	Added information about conformal coating. Updated pictures of GND planes in chapter 3.
2022-03-07	1.4	Updated chapter 3 on PCB routing.

Disclaimer

The information herein is believed to be correct as of the date issued. Acconeer AB ("**Acconeer**") will not be responsible for damages of any nature resulting from the use or reliance upon the information contained herein. Acconeer makes no warranties, expressed or implied, of merchantability or fitness for a particular purpose or course of performance or usage of trade. Therefore, it is the user's responsibility to thoroughly test the product in their particular application to determine its performance, efficacy and safety. Users should obtain the latest relevant information before placing orders.

Unless Acconeer has explicitly designated an individual Acconeer product as meeting the requirement of a particular industry standard, Acconeer is not responsible for any failure to meet such industry standard requirements.

Unless explicitly stated herein this document Acconeer has not performed any regulatory conformity test. It is the user's responsibility to assure that necessary regulatory conditions are met and approvals have been obtained when using the product. Regardless of whether the product has passed any conformity test, this document does not constitute any regulatory approval of the user's product or application using Acconeer's product.

Nothing contained herein is to be considered as permission or a recommendation to infringe any patent or any other intellectual property right. No license, express or implied, to any intellectual property right is granted by Acconeer herein.

Acconeer reserves the right to at any time correct, change, amend, enhance, modify, and improve this document and/or Acconeer products without notice.

This document supersedes and replaces all information supplied prior to the publication hereof.